



Contents lists available at ScienceDirect



Efficiency of photosynthesis in a Chl *d*-utilizing cyanobacterium is comparable to or higher than that in Chl *a*-utilizing oxygenic species

S.P. Mielke ^{a,b,*}, N.Y. Kiang ^a, R.E. Blankenship ^{c,d}, M.R. Gunner ^e, D. Mauzerall ^b^a NASA Goddard Institute for Space Studies, Columbia University, New York, NY, USA^b Laboratory of Photobiology, Rockefeller University, New York, NY, USA^c Department of Biology, Washington University, St. Louis, MO, USA^d Department of Chemistry, Washington University, St. Louis, MO, USA^e Physics Department, City College of New York, New York, NY, USA

ARTICLE INFO

Article history:

Received 6 May 2011

Received in revised form 9 June 2011

Accepted 13 June 2011

Available online 25 June 2011

Keywords:

Acaryochloris marina

Oxygenic photosynthesis

Energy-storage efficiency

Photoacoustics

ABSTRACT

The cyanobacterium *Acaryochloris marina* uses chlorophyll *d* to carry out oxygenic photosynthesis in environments depleted in visible and enhanced in lower-energy, far-red light. However, the extent to which low photon energies limit the efficiency of oxygenic photochemistry in *A. marina* is not known. Here, we report the first direct measurements of the energy-storage efficiency of the photosynthetic light reactions in *A. marina* whole cells, and find it is comparable to or higher than that in typical, chlorophyll *a*-utilizing oxygenic species. This finding indicates that oxygenic photosynthesis is not fundamentally limited at the photon energies employed by *A. marina*, and therefore is potentially viable in even longer-wavelength light environments.

© 2011 Elsevier B.V. All rights reserved.

1. Introduction

Discovered in 1996 [1], the cyanobacterium *Acaryochloris marina* is the only photosynthetic species known to employ chlorophyll (Chl) *d* as its main photopigment. Because the peak absorbance band of Chl *d* is redshifted ≈ 40 nm *in vivo* relative to that of Chl *a*, and despite the resulting $\approx 0.1\text{-eV}$ loss in energy of the exciting photon, this organism is able to perform oxygenic phototrophy in niche-environments enriched in far-red light [2,3]. Prior to the discovery of *A. marina*, it was broadly assumed that all oxygenic species employ strictly Chl *a* for primary photochemistry, owing to the stringent energy requirements of water oxidation [4,5]. In *Acaryochloris* reaction centers (Photosystems (PS) I and II), with the possible exception of the P_{D1} chlorophyll in PSII [6–9], Chl *a* is replaced by Chl *d*, increasing the solar photon flux available to the organism for O₂-evolving photosynthesis by $\approx 15\%$ [10]. Elucidating photochemistry in this species is therefore of wide-ranging scientific interest. From the viewpoint of basic photosynthesis research, doing so will address the fundamental biomolecular, kinetic, and thermodynamic requirements for the difficult reaction in which water is oxidized and molecular oxygen released. From the viewpoint of renewable energy research, insights on photosynthesis in *A. marina* potentially inform the design of efficient solar fuel production devices predicated on natural systems [11]. We note that a new chlorophyll,

Chl *f*, with peak absorbance further redshifted by 5–7 nm *in vitro* relative to that of Chl *d*, was recently discovered in cyanobacterial communities under far-red light, but its associated organism and role have not yet been determined [12].

Spectroscopic studies have suggested that the excitation wavelengths of the primary electron donors in *A. marina* lie at approximately 740 nm in PSI [13,14] and 713 nm in PSII [15], leading to the designations P740 and P713, respectively, for those pigments. The corresponding wavelengths in Chl *a* species lie at 700 nm (PSI) and 680 nm (PSII), representing, in both cases, a photon energy 5% higher than that in *A. marina*. This has led to speculation that, without some compensatory adjustment to oxygenic photochemistry, *Acaryochloris* might be limited by the lower excitation energies of its reaction centers. With a redder and therefore lower-energy photon absorbed, the primary electron donor must either be a poorer oxidant and/or the excited state must be a poorer reductant. In particular, PSII represents the most powerful oxidant in biology, with an electrochemical midpoint potential of ≈ 1.2 V [16–18]. The question of how PSI and PSII in *A. marina* cope with the smaller initial energy has motivated numerous studies of redox chemistry in this organism [e.g., 6–8,19–23]. However, to date, no direct measurements of photosynthetic energy-storage in *A. marina* have been reported. Determining the efficiency of energy-storage, and comparing with that in Chl *a*-utilizing organisms, directly addresses whether photosynthesis in *A. marina* is fundamentally limited at excitation wavelengths longer than 700 nm. By extension, doing so also addresses whether oxygenic photochemistry generally is thus limited.

* Corresponding author at: NASA Goddard Institute for Space Studies, Columbia University, New York, NY, USA. Tel.: +1 212 327 8217.

E-mail address: smielke@giss.nasa.gov (S.P. Mielke).

Here, we report direct measurements of energy storage in *A. marina*, and compare our results with those obtained from Chl *a*-utilizing species to determine differences in the efficiency of oxygenic photosynthesis. Measurements were carried out using millisecond-timescale photoacoustic (PA) spectroscopy. PA methods provide fast and accurate thermodynamic information by detecting the heat dissipated (E_{dis}) by a photosynthetic sample on illumination with laser pulses of known wavelength and flux [24–27] (see Section 2). This allows direct measurement of the energy-storage efficiency, ϵ , defined as the ratio of energy stored in products of photochemistry (E_{sto}) to the photon energy absorbed (E_{abs}):

$$\epsilon \equiv E_{\text{sto}} / E_{\text{abs}} = (E_{\text{abs}} - E_{\text{dis}}) / E_{\text{abs}} \quad (1)$$

Our results indicate that the maximal energy-storage efficiency of photosynthesis in *A. marina* is comparable to or even slightly higher than that in Chl *a* organisms, and therefore that the former is not limited by the lower trap energies characteristic of its Chl *d*-utilizing reaction centers.

2. Materials and methods

2.1. Cell growth

Acaryochloris marina, strain MBIC11017, was grown in BG-11 medium at 28 °C with continuous agitation (100 rpm) [3]. Continuous light was provided by an incandescent bulb at an average intensity of 15 $\mu\text{E m}^{-2} \text{s}^{-1}$, photosynthetically active radiation (PAR). *Synechococcus leopoliensis* (UTEX 625) was grown in Allen's medium at 21 °C with continuous agitation (100 rpm). Continuous light was provided by four fluorescent bulbs at an average intensity of 50 $\mu\text{E m}^{-2} \text{s}^{-1}$ PAR. We used log phase cells containing 3–7 µg chlorophyll ml⁻¹ medium for which the batch-averaged efficiency, $\langle \epsilon_{\text{max}} \rangle$, was 40 ± 3% (*Acaryochloris*) and 32 ± 3% (*Synechococcus*), where the errors are rms deviations. Cultures that fell outside this range (≈ 5% of all observed) were deemed to exceed normal batch-to-batch variation, and were not used.

2.2. Sample preparation and absorbance spectra

For both *A. marina* and *S. leopoliensis*, cells were affixed under mild vacuum to filters (HAWP04700, 0.45 µm pore size, Millipore) cut to 1.4 cm diameter. 1 ml medium containing 3 mM NaHCO₃ was added to 1 ml cell culture for filtration, yielding samples containing 3–7 µg chlorophyll, for which photoacoustic signals were both reproducible and proportional to laser energy. Filtration was stopped prior to the liquid level being drawn off the filter, so that samples remained wet. Absorbance spectra (Fig. 1) of entire samples (cells and bicarbonate medium on filters) were obtained using an Olis spectrophotometer.

2.3. Photoacoustic (PA) measurements

Samples were placed in a PA cell [26] and illuminated using an Optical Parametric Oscillator (OPO) (Uniwave Technology) pumped by a 532 nm flash lamp-pumped Nd:YAG laser (SureliteII, Continuum) with 5-ns pulses at a frequency of 3.33 Hz. Pulse wavelength was measured using an SD2000 spectrometer (Ocean Optics). The FWHM wavelength of the pulses was <2 nm. The OPO output, after removal of green light, was attenuated in steps by neutral density filters. Light pulses were led to the sample via a liquid lightguide (S2000, Newport). Incident pulse energies were measured with an energy sensor (J3-09, Coherent) and joulemeter (JD2000, Coherent). Continuous, 35 W background light with IR removed (sufficient to saturate but not heat the samples) was supplied via fiber optic cable by a lamp and DC power supply (GPR-1810HD, GWInsteek). The PA cell was suspended by viscoelastic supports to provide isolation from external vibrations.

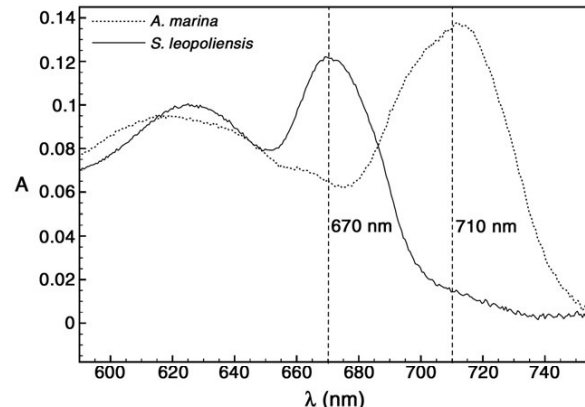


Fig. 1. Absolute absorbance between wavelengths (λ) 590 and 755 nm for whole samples (cells on filter substrate) containing *S. leopoliensis* (solid curve) and *A. marina* (dotted curve) intact cells. Wavelengths of maximum chlorophyll absorbance, 670 nm and 710 nm, respectively (indicated by dashed lines), were used in the corresponding PA experiments. Note that the absorbance of the samples is small; i.e., they are optically thin.

Pressure changes within the cell following laser pulses were detected by a microphone (BL-1785, Knowles), whose output was amplified 100-fold using a low-noise preamplifier (Model 1201, Ithaco) with low- and high-pass filters set at 300 Hz and 3 Hz, respectively. The signal from the preamplifier was digitized by an 8-bit oscilloscope (TDS540, Tektronix) collecting 500 points per trace. Energy and PA data were acquired, averaged over 400 to 1600 flashes, and digitally transferred to a Dell PC for analysis using Matlab.

For each sample, an averaged PA trace and pulse energy were obtained first in the dark and then in the presence of continuous background light. Pulse wavelengths were set at 670 nm or 710 nm to correspond with chlorophyll absorbance maxima for *S. leopoliensis* or *A. marina*, respectively (Fig. 1). Background light saturates photosynthetic activity so that all absorbed laser energy, E_{abs} (Eq. (1)), is degraded to heat, generating a pressure wave (proportional to the rate of heat release) within the PA apparatus that is detected by the microphone, resulting in a signal with amplitude, S_{lt} (Fig. 2). When only laser pulses excite the sample, some of the absorbed light, E_{sto} , is used for photosynthesis, and less heat is released, resulting in a smaller

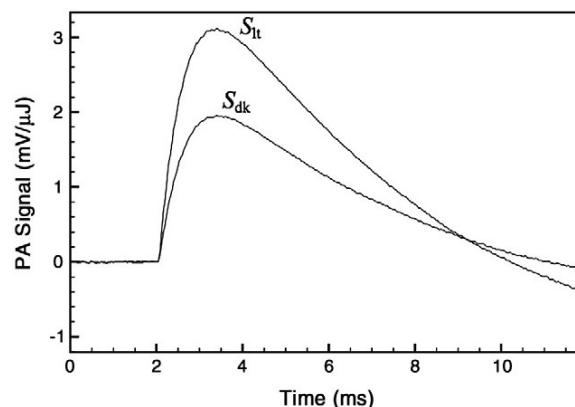


Fig. 2. Representative PA signals. S_{dk} and S_{lt} are the amplitudes (in mV/µJ) of averaged signals from a dark-adapted, active *A. marina* sample (0.8 cm²), and a sample under continuous saturating light, respectively, here at a laser pulse energy of 4.8 µJ ($\lambda = 710$ nm). The pulses flash the sample at 2.05 ms (x-axis), and the peaks of the resulting pressure wave, corresponding to S_{dk} and S_{lt} , are detected by a microphone at 3.4 ms. Signals from the microphone are amplified, and displayed as time-dependent voltages by an oscilloscope (see Materials and methods). The energy-storage efficiency at this energy calculated from the amplitudes (Eq. (2)) is $\epsilon_{4.8 \mu\text{J}} = 38\%$. These data correspond to the measurement at 4.8 µJ shown in Fig. 3A.

signal with amplitude, S_{dk} , allowing the energy-storage efficiency, ε , at a chosen energy to be calculated using Eq. (2) (Section 3). Values of S_{dk} and S_{lt} used for the calculations were obtained by averaging over data points centered at the maximum value of the corresponding averaged signal. A small ($0.1 \text{ mV}/\mu\text{J}$) contribution from the filter substrate was subtracted from all measured amplitudes. The efficiency decreases linearly with increasing energy at low energies [25,26], allowing ε_{\max} to be calculated by extrapolation to zero energy of a linear fit to a set of low-energy measurements (Fig. 3). The range of low energies over which ε is linear is organism-specific, and was determined by obtaining measurements out to energies where the samples were fully saturated by the flashes ($\varepsilon \approx 0$) (data not shown).

3. Results

The PA experiments reported here provide the millisecond-timescale energy-storage efficiency in *A. marina* and *Synechococcus leopoliensis* intact cells, using laser pulses of wavelength 710 nm and 670 nm, respectively—the wavelengths of maximum chlorophyll absorbance in the corresponding samples (Fig. 1), where both photosystems contribute to energy storage [25]. *S. leopoliensis* was chosen as the control species because of its similarity to cyanobacteria used in our previous measurements [26]. It is assumed to be generally representative of Chl *a* cyanobacteria.

Millisecond-timescale PA studies employing intact cells capture the *in vivo* efficiency of the essentially complete light reactions of

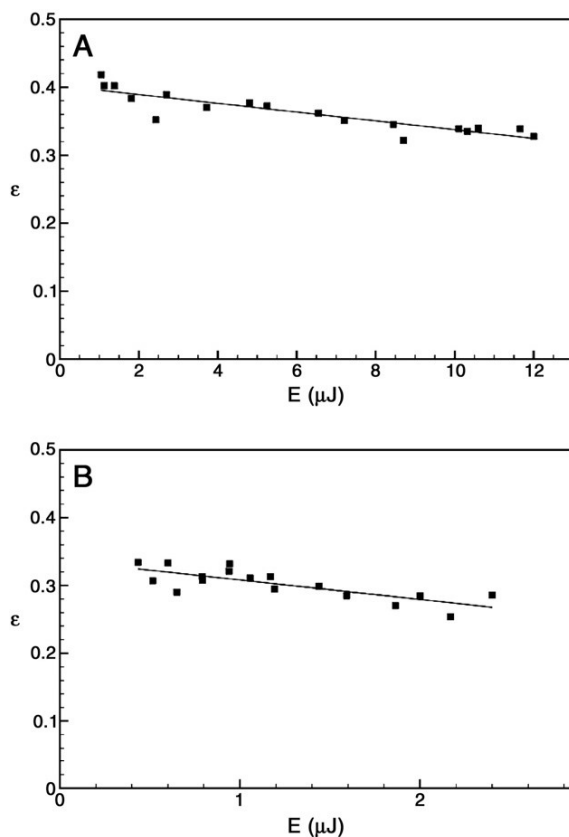


Fig. 3. Energy-storage efficiency, ε , as a function of laser pulse energy incident on samples containing (A) *A. marina* intact cells (pulse wavelength, $\lambda = 710 \text{ nm}$); and (B) *S. leopoliensis* intact cells (pulse wavelength, $\lambda = 670 \text{ nm}$). At low pulse energies, ε decreases linearly with increasing energy, so the maximal efficiency at chosen λ , ε_{\max} , is obtained from the y -intercept of a linear fit to efficiencies measured over a range of low energies. For *A. marina*, $\varepsilon_{\max} = 40 \pm 1\%$, and for *S. leopoliensis*, $\varepsilon_{\max} = 34 \pm 1\%$. The data point at $4.8 \mu\text{J}$ in Fig. 3A corresponds to the data shown in Fig. 2.

photosynthesis, likely representing electron transfer from water to NADP to form predominantly NADPH and O_2 [25,28]. Carbon fixation occurs on a longer timescale of seconds. Fig. 2 shows a set of PA measurements (see Section 2) from the present investigation, obtained from an *A. marina* sample at a flash energy of $4.8 \mu\text{J}$ ($\lambda = 710 \text{ nm}$). The abscissa in Fig. 2 corresponds to time in milliseconds, and the ordinate to the energy-normalized PA signals in $\text{mV}/\mu\text{J}$, with S_{dk} denoting the amplitude of the signal from the dark-adapted sample, and S_{lt} that of the signal from the light-saturated sample. In the latter, $E_{sto} \approx 0$, so that $E_{abs} \approx E_{dis}$ (see Section 1); i.e., none of the absorbed flash energy is stored, and so is all dissipated as heat through quenching mechanisms, at the level of the antenna, that are employed by photosynthetic organisms when the reaction center traps are closed [16]. In the dark-adapted sample, some of the absorbed energy is stored by flash-initiated photochemistry, so less heat is released. The efficiency at the chosen pulse energy is then obtained directly from the PA signals (see Eq. (1)):

$$\varepsilon = 1 - E_{dis} / E_{abs} = 1 - S_{dk} / S_{lt}. \quad (2)$$

The maxima of the PA signals are used to calculate the ratio of the dark to the light signal because this maximizes the signal-to-noise, while capturing linear dependence of the ratio on flash energy; in particular, the difference between ratios obtained directly from the PA signals and those obtained from time integrals of the signals is less than the experimental error (data not shown) [27]. For the signals in Fig. 2, $S_{dk} = 1.95 \text{ mV}/\mu\text{J}$ and $S_{lt} = 3.08 \text{ mV}/\mu\text{J}$. From these values, a small correction of $0.1 \text{ mV}/\mu\text{J}$ for saturation-independent contribution to the signals from the sample substrate was subtracted (see Section 2), yielding $\varepsilon_{4.8 \mu\text{J}} = 1 - 0.621 = 0.379$.

Results from PA measurements of the energy-storage efficiency in both *A. marina* and *S. leopoliensis* as a function of laser flash energy are shown in Fig. 3. The efficiencies decrease with increasing energy, because the flashes themselves begin to saturate the photosystems. This decrease is linear in the energy range used (Materials and methods), allowing the maximal efficiency, ε_{\max} , to be obtained from the y -intercept of a linear fit to a set of low-energy measurements ($\varepsilon_{\max} = \lim_{E_{abs} \rightarrow 0} \varepsilon$). Fits to the data in Fig. 3 (solid lines), yield, for *A. marina* at 710 nm , $\varepsilon_{\max} = 40 \pm 1\%$ (Fig. 3A), and, for *S. leopoliensis* at 670 nm , $\varepsilon_{\max} = 34 \pm 1\%$ (Fig. 3B). These results indicate that the efficiency of ms-timescale photochemistry in the Chl *d*-containing cyanobacterium is $\approx 6\%$ higher than that in the Chl *a*-containing cyanobacterium.

4. Discussion

4.1. *A. marina* and the Z-scheme of oxygenic photosynthesis

In oxygenic photosynthesis, photo-excitation of the two redox-coupled photosystems, PSI and PSII, mediates the transfer of electrons from H_2O to NADP in the light reactions, yielding molecular oxygen, and ultimately carbohydrate (by reduction of CO_2) in the dark reactions. The redox potentials driving electron transfers in the reaction,



are commonly represented as the “Z-scheme” (Fig. 4), in which the primary electron-donor photo-excitations are shown as redox spans allowing thermodynamically downhill electron-transfer [29]. Because overall transfer from H_2O to NADP^+ occurs on a timescale of milliseconds [18,28], ms-timescale photoacoustic measurements employing intact cells are well-suited for measuring the efficiency of reaction (3). The pulse frequency of 3 Hz used here (Section 2) is appropriate for capturing completion of the reaction for each PA signal obtained.

In Fig. 4, H_2O , NADP, and the primary donor ground-states, P680 and P700, are shown at their respective standard-state (pH 7)

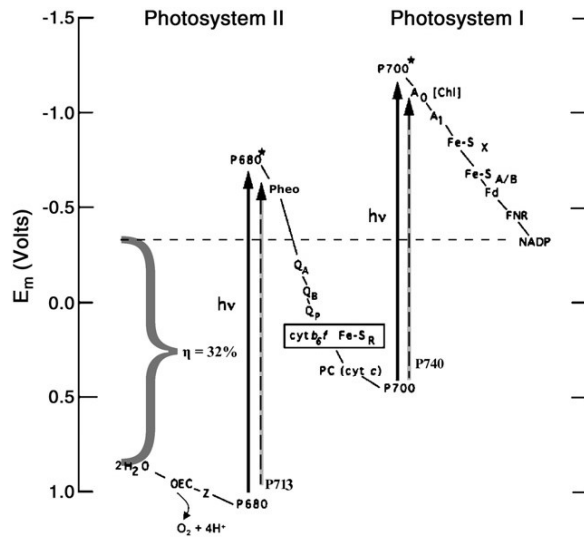


Fig. 4. Z-scheme of oxygenic photosynthesis. Solid and dashed arrows represent, respectively, the changes in midpoint redox potential (E_m) generated by photo-excitation of the primary donors in Chl *a* organisms (P680 in PSII and P700 in PSI), and in *Acaryochloris marina* (P713 in PSII and P740 in PSI). Because the ground- and excited-state potentials of the latter are not well known, the placement of the dashed arrows is somewhat arbitrary. In Chl *a* species, the estimated maximum efficiency (η) of the overall reaction that oxidizes water and reduces NADP is indicated by the bracket, and is $\approx 32\%$ of the total excitation energy of 3.60 eV, the sum of $h\nu = 1.83$ eV for a 680-nm photon and 1.77 eV for a 700-nm photon. In *A. marina*, the corresponding efficiency is $\approx 33\%$, because both excitations are $\approx 5\%$ lower in energy.

midpoint redox potentials, E_m^0 (vertical axis). Photo-excitations of P680 and P700 to the excited states, P680* and P700*, are indicated by solid arrows that span the resulting potential changes, corresponding to the energies ($h\nu$) of 680- and 700-nm photons. We note that care should be exercised when invoking this model, since the actual excitation (singlet-state) energies are not equivalent to the associated changes in free energy (ΔG) relevant to redox chemistry. Here, to be consistent with convention, we assume the entropy change upon excitation is negligible, so that $h\nu \approx \Delta G^0 \approx \Delta H^0$, where ΔH^0 is the standard-state enthalpy change. Also shown in Fig. 4 at their respective midpoint potentials are the oxygen-evolving complex (OEC), and electron-transport cofactors, indicated by their abbreviations; e.g., Pho (pheophytin) and Q (quinone). The potential difference between water ($E_m^0 = 0.816$ V) and NADP ($E_m^0 = -0.324$ V, indicated by a dashed line) is shown by a gray bracket, and has the value, $\Delta E_m^0 = 1.14$ V [16]. We point out that both water and NADP represent highly concentration- and pH-dependent redox couples, and reiterate that these are standard-state values obtained at pH 7. It is of interest that PA experiments, which capture purely the enthalpy, are not affected by the ratio of reductant to oxidant, or Nernst ratio, which is an entropic contribution to the free energy and does not affect the enthalpy. Because they are normalized to a mole of photons, the measurements reported here refer to the standard molar enthalpy.

As a point of reference for the present results, an idealized estimate of the maximal energy-storage efficiency of photosynthesis, η , can be obtained by calculating the fraction of the combined excitation energies used to transfer an electron from H_2O to NADP:

$$\eta = e\Delta E_m^0 / (hc/\lambda_{PSI} + hc/\lambda_{PSII}). \quad (4)$$

Here, e is an integer unit of electron charge, $\Delta E_m^0 = 1.14$ V is the standard-state midpoint potential difference resulting from the transfer of one electron from water to NADP, and hc/λ_{PSI} and hc/λ_{PSII} are the excitation energies of the PSI and PSII primary donors, where h is Planck's constant, c is the speed of light, and λ_{PSI} , λ_{PSII} are the

respective excitation wavelengths. For P700 and P680, these energies are $hc/\lambda_{700\text{ nm}} = 1.77$ eV and $hc/\lambda_{680\text{ nm}} = 1.83$ eV. The estimated maximum efficiency of energy storage per two photons is then, $\eta = 1.14\text{ eV}/3.60\text{ eV} = 0.317$. Assuming all electrons removed from water by the two-photon process are used to reduce NADP, the total efficiency of the eight-photon process represented by reaction (3) is also $\approx 32\%$. This analysis assumes unity quantum yield (i.e., that all excited states result in a charge-separated state).

In Fig. 4, the dashed arrows represent photo-excitations of Chl *d* primary donors in the PSI and PSII reaction centers of *A. marina*, corresponding to those at 700 nm and 680 nm, respectively, in Chl *a* species (solid arrows in the figure). At the commonly accepted wavelengths inferred from spectroscopic data, the excitation energies are 1.68 eV for P740*, and 1.74 eV for P713*, both 5% smaller than the corresponding Chl *a* energies. Assuming the products of photosynthesis in *A. marina* are the same as those in Chl *a* organisms – in particular, that ms-timescale photosynthesis is described by reaction (3) – one can approximate the maximal energy-storage efficiency using Eq. (4): $\eta = 1.14\text{ eV}/(hc/\lambda_{PSI} + hc/\lambda_{PSII}) = 0.333$. Here, 1.14 eV is again the energy change, per two photons, associated with moving one electron through the potential difference separating H_2O and NADP; and hc/λ_{PSI} , hc/λ_{PSII} are now the above excitation energies of P740* and P713*. This estimate suggests, consistent with the present results, that photosynthetic efficiency in *A. marina* might be slightly higher than that in Chl *a* species, based simply on its making equivalent use of less captured energy (assuming the quantum yield is unchanged).

We find that the maximal energy-storage efficiency, ε_{max} , in *A. marina* is $40 \pm 1\%$, and that in the cyanobacterium, *S. leopoliensis*, is $34 \pm 1\%$. Previous photoacoustic investigations of ms-timescale energy-storage in intact cells of the alga, *Chlorella vulgaris*, have reported that $\varepsilon_{max} = 43 \pm 2\%$ [25]. These values are consistent with the estimates obtained above, but inherently reflect losses and excess storage characteristic of natural systems that are not considered by Eq. (4). In particular, Eq. (4) likely underestimates the efficiency by neglecting storage associated with the proton gradient generated by the vectorial proton loss in reaction (3), and with subsequent formation of ATP [16,18]. Our measurement of $\varepsilon_{max} = 34 \pm 1\%$ in *Synechococcus*, in close agreement with, but slightly higher than, the estimate of 32%, is consistent with this conclusion. The contribution of proton transport to energy storage likely depends, for example, on light intensity, but could be significant even at low intensities, and is likely substantial at higher intensities. Future efforts will aim to quantify this contribution; e.g., by repeating the PA measurements in the presence of an uncoupler. More generally, our finding that the enthalpic efficiency is higher than the ideal free energy efficiency – by $\approx 7\%$ in *A. marina* – implies entropic contributions are not negligible, and may be 15% or more of the measured efficiency.

Loss processes not considered by Eq. (4) include fluorescence (generally negligible, although not in the case of *Chlorella* [25]), and excitation transfer from antennae pigments to the reaction centers. We estimate excitation transfer losses inherent to the experiments reported here are $\approx 2\%$, assuming the *Synechococcus* traps lie at 680 and 700 nm, and the *Acaryochloris* traps at 713 and 740 nm (these remain to be precisely determined). A higher efficiency in *A. marina* than in Chl *a* organisms resulting from its equivalent use of lower trapped energies will likely be difficult to resolve experimentally (the difference predicted above is less than 2%). The $\approx 6\%$ difference with respect to *Synechococcus* seen here might indicate, for instance, relatively significant ATP production (or some other mode of storage) associated with photosynthesis in *Acaryochloris* and *Chlorella*, at least in the cell cultures investigated.

The dashed arrows in Fig. 4 are drawn 5% shorter than the solid arrows to reflect the 5% energy difference between P713* and P680*, and between P740* and P700*. Because the precise values of the midpoint potentials of the ground states P713/P713⁺ and P740/P740⁺ are not known, the placement of the dashed arrows is

somewhat arbitrary. However, the extent to which these potentials can vary with respect to those of P680/P680⁺ and P700/P700⁺ is restricted by the potential differences required for efficient transfer of electrons to P713⁺ from H₂O, via the OEC and redox-active tyrosine (Z in Fig. 4) (i.e., PSII donor side); the reduction of P740⁺ initiated from P713* via the cytochrome b₆f complex (cyt b₆—Fe—S_R) (i.e., PSII acceptor side/PSI donor side); and to NADP⁺ from P740* (i.e., PSI acceptor side). Evidence indicates that the *Acaryochloris* ground-state oxidative potentials are likely close to those of P700 (≈ 0.51 V) and P680 (≈ 1.2 V) [14,20–23]. For PSII, this is consistent with the need for a potential difference (≈ 0.4 V overpotential [30]) needed to oxidize H₂O at a finite rate, and with evidence that the PSII donor-side potentials are essentially unchanged [19,20]. (We note that Cser et al. have reported a 45 mV decrease in the potential of redox-active tyrosine in *Acaryochloris* relative to that in *Synechocystis* [7].)

If ground-state $E_{\text{mP713}}^{\circ} \approx E_{\text{mP680}}^{\circ}$, and the potential changes, ΔE_{m} , for the transitions P713 → P713* and P680 → P680* are 1.74 V and 1.83 V, respectively, P713* would be ≈ 90 mV less reducing than P680*. Depending on the midpoint potential of the primary acceptor pheophytin a (Pheo), E_{mPheo}° , the primary redox reaction P713*Pheo → P713⁺Pheo[−] might even require thermodynamically uphill electron transfer. Such an alteration of the redox properties of the primary donor and acceptor could potentially inhibit photosynthesis by adversely affecting the quantum yield. (The same is true of PSI, though here, for purposes of illustration, we focus on PSII, the potentials of which are likely more rigidly constrained by the requirements of water oxidation [21,22].) However, it is possible that *A. marina* has required no significant adaptations of photochemistry in PSII, beyond incorporation of Chl d, to preserve the efficacy of photosynthesis in its light environments. As long as the subsequent stages of electron transfer from Pheo[−] to the quinone remain sufficiently exergonic, even a modestly endergonic step to reduce Pheo may not lead to significant loss of product [31].

Alternatively, *Acaryochloris* might have compensated for inhibitory changes in redox properties by adapting the protein environment of its photosystems to alter the midpoint potentials of electron-transport cofactors. Allakhverdiev et al. [23] (also see Ref. [32]) have proposed that the change in E_{mP713}° relative to E_{mP680}° has been compensated by an ≈ 60 mV shift of E_{mPheo}° from -536 ± 8 mV (*Synechocystis*) to -478 ± 24 mV (*Acaryochloris*), preserving the potential difference with respect to P713* needed for efficient primary charge separation. Based on this shift, the authors estimate E_{m}° of P713⁺ to be 1.18 V, which would slightly reduce the driving force for oxidation of the OEC relative to that of P680⁺ ($E_{\text{m}}^{\circ} \approx 1.2$ V). As these authors and others [7, M. Dong, et al. (in preparation)] point out, significant shifts in the value of E_{mPheo}° cannot be explained by a change in the proximal environment of the cofactor. There is 85% sequence identity between the active D1 subunit in PSII of *A. marina* [3] and that in other cyanobacteria, and no evidence for a nearby mutation that would alter the electrostatic or hydrogen-bonding properties of Pheo a in D1 [7,23, M. Dong, et al. (in preparation)]. It has been proposed that hydrophobic or longer-range electrostatic interactions might affect the value of E_{mPheo}° in D1 [23], but the distal protein environment in *A. marina* is also very similar to that in other cyanobacteria. The sequence of the D2 subunit is 88% identical to that of *T. elongatus*. A significant shift in the midpoint potential of Pheo in *Acaryochloris* is also inconsistent with multi-conformation continuum electrostatics (MCCE) [33] calculations based on an *A. marina* PSII model structure, which suggest the change with respect to the Chl a system, if any, is small, and possibly toward lower (more negative) potential [M. Dong, et al. (in preparation)].

Another possibility, for which some evidence has been presented [6–9], is that the primary donor in PSII of *A. marina* is not the special pair Chl d, P713, but rather the D1-side monomer (accessory) Chl d, Chl_{D1}, and, moreover, that the D1-side special pair chlorophyll is not Chl d at all, but rather remains Chl a; i.e., the special pair is a Chl a/d

heterodimer, rather than a Chl d/d homodimer. Even in strictly Chl a systems, there is still debate on whether P680 or Chl_{D1} acts as primary donor to Pheo a [17,34,35]. In *A. marina*, the proposed scenario [6–9] is that photon energy absorbed by Chl d-dominated antennae is preferentially funneled to a Chl d occupying the Chl_{D1} site, initiating charge separation. The potential of this pigment relative to that of a Chl a occupying the P_{D1} site (i.e., P680) and Pheo a leads to electron transfer from the excited Chl_{D1}* to Pheo a, followed by oxidation of P_{D1} by Chl_{D1}⁺, and of the OEC by P_{D1}⁺. (Potentials of Chl d, Chl a, and Pheo a in vitro have been reported to be +0.88, +0.81, and +1.14 V, respectively [36].) This process would result in a charge-separated state stabilized by the same Chl a/Pheo a redox couple as in typical oxygenic species. Further investigation is needed to determine the full extent and nature of adaptations of photochemistry in *A. marina*. However, this scenario is consistent with the organism having minimally altered the oxygenic reaction center in order to employ Chl d antennae to accommodate far-red light environments, an interpretation supported by the aforementioned high sequence identity between its reaction center proteins and those of other cyanobacteria.

5. Conclusions

In conclusion, we find the *in vivo* energy-storage efficiency of oxygenic photosynthesis in *A. marina* is comparable to or higher than that in species that employ strictly Chl a in primary photochemistry. This clearly demonstrates that: (1) the energy-use efficiency of photosynthesis in *Acaryochloris* is not limited by the photon energy at wavelengths ≈ 40 nm longer than those utilized by other oxygenic organisms; and therefore (2) oxygenic photochemistry generally is not fundamentally limited at these wavelengths, and so is likely viable in even redder light environments, such as those that might be inhabited by Chl f-utilizing species [12]. These conclusions are consistent with the simple observation that a 5% decrease in energy of the excited reaction centers is relatively small compared to the $\approx 65\%$ loss from the ensuing electron transfers from water to NADP, which is required by irreversible thermodynamics in both Chl a and d systems. In ongoing studies of *A. marina*, we seek to measure the energy-storage efficiency at wavelengths longer than 710 nm to investigate further the minimal energy requirements of oxygenic photosynthesis; and to isolate the contributions of PSI and PSII to energy storage, both on the ms-timescale of the present study, and, by using isolated and purified reaction centers, on the ns–μs-timescale of electron transfer. Taken together, results of this effort may additionally allow identification of what (if any) adaptations of oxygenic photosynthesis *A. marina* has employed beyond use of Chl d; and determination of the precise trap wavelengths of both photosystems.

Acknowledgments

We are grateful to Irena Zielinski-Large for technical support; Mr. Xianglu Li and Dr. Min Chen for critical advice on culturing *Acaryochloris marina*; Prof. Shmuel Malkin and Dr. Minghui Dong for helpful discussions; the NASA Astrobiology Institute, Dr. Carl Pilcher, and Prof. Victoria Meadows for support by a NASA Postdoctoral Program fellowship and Director's Discretionary Fund grant. This research is partially supported by the Photosynthetic Antenna Research Center (PARC), an Energy Frontier Research Center funded by the DOE, Office of Science, Office of Basic Energy Sciences under Award Number DE-SC 0001035. REB also thanks the Exobiology program of NASA for support under grant number NNX08AP62G. MRG acknowledges DOE Grant DE-SC 0001423 and infrastructure support from the NIH Grant 5G12 RR03060.

References

- [1] H. Miyashita, H. Ikemoto, N. Kurano, K. Adachi, M. Chihara, S. Miyachi, Chlorophyll d as a major pigment, *Nature* 383 (1996) 402.

- [2] A.W.D. Larkum, M. Kühl, Chlorophyll d: the puzzle resolved, *Trends Plant Sci.* 10 (2005) 355–357.
- [3] W.D. Swingley, et al., Niche adaptation and genome expansion in the chlorophyll d-producing cyanobacterium *Acaryochloris marina*, *Proc. Natl. Acad. Sci. USA* 105 (2008) 2005–2010.
- [4] D. Mauzerall, Why chlorophyll? *Ann. New York Acad. Sci.* 206 (1973) 483–494.
- [5] L.O. Björn, G.C. Papageorgiou, R.E. Blankenship, Govindjee, Why Chl a? A viewpoint, *Photosynth. Res.* 99 (2009) 85–98.
- [6] E. Schlodder, et al., Both chlorophylls a and d are essential for the photochemistry in photosystem II of the cyanobacteria, *Acaryochloris marina*, *Biochim. Biophys. Acta* 1767 (2007) 589–595.
- [7] K. Cser, et al., Energetics of Photosystem II charge recombination in *Acaryochloris marina* studied by thermoluminescence and flash-induced chlorophyll fluorescence measurements, *Photosynth. Res.* 98 (2008) 131–140.
- [8] T. Renger, E. Schlodder, The primary electron donor of photosystem II of the cyanobacterium *Acaryochloris marina* is a chlorophyll d and the water oxidation is driven by a chlorophyll a/chlorophyll d heterodimer, *J. Phys. Chem. B* 112 (2008) 7351–7354.
- [9] T. Renger, E. Schlodder, Primary photophysical processes in photosystem II: bridging the gap between crystal structure and optical spectra, *Chem. Phys. Chem.* 11 (2010) 1141–1153.
- [10] M. Chen, R.E. Blankenship, Expanding the solar spectrum used by photosynthesis, *Trends Plant Sci.* (2011), doi:10.1016/j.tplants.2011.03.011.
- [11] N.S. Lewis, D.G. Nocera, Powering the planet: chemical challenges in solar energy utilization, *Proc. Natl. Acad. Sci. USA* 103 (2006) 15729–15735.
- [12] M. Chen, et al., A red-shifted chlorophyll, *Science* 329 (2010) 1318–1319.
- [13] Q. Hu, et al., A photosystem I reaction center driven by chlorophyll d in oxygenic photosynthesis, *Proc. Natl. Acad. Sci. USA* 95 (1998) 13319–13323.
- [14] T. Tomo, et al., Characterization of highly purified photosystem I complexes from the chlorophyll d-dominated cyanobacterium *Acaryochloris marina* MBIC 11017, *J. Biol. Chem.* 283 (2008) 18198–18209.
- [15] T. Tomo, T. Okubo, S. Akimoto, M. Yokono, H. Miyashita, T. Tsuchiya, T. Noguchi, M. Mimuro, Identification of the special pair of photosystem II in a chlorophyll d-dominated cyanobacterium, *Proc. Natl. Acad. Sci. USA* 104 (2007) 7283–7288.
- [16] R.E. Blankenship, Molecular Mechanisms of Photosynthesis, Blackwell, Oxford, 2002.
- [17] F. Rappaport, B.A. Diner, Primary photochemistry and energetics leading to the oxidation of the (Mn)4Ca cluster and to the evolution of molecular oxygen in photosystem II, *Coord. Chem. Rev.* 252 (2008) 259–272.
- [18] H. Dau, I. Zaharieva, Principles, efficiency, and blueprint character of solar-energy conversion in photosynthetic water oxidation, *Acc. Chem. Res.* 42 (2009) 1861–1870.
- [19] M. Reza Razeghifard, et al., Spectroscopic studies of photosystem II in chlorophyll d-containing *Acaryochloris marina*, *Biochemistry* 44 (2005) 11178–11187.
- [20] D. Shevela, et al., Characterization of the water oxidizing complex of photosystem II of the Chl d-containing cyanobacterium *Acaryochloris marina* via its reactivity towards endogenous electron donors and acceptors, *Phys. Chem. Chem. Phys.* 8 (2006) 3460–3466.
- [21] M. Schenderlein, M. Çetin, J. Barber, A. Telfer, E. Schlodder, Spectroscopic studies of the chlorophyll d containing photosystem I from the cyanobacterium, *Acaryochloris marina*, *Biochim. Biophys. Acta* 1777 (2008) 1400–1408.
- [22] B. Baileul, et al., The thermodynamics and kinetics of electron transfer between cytochrome b6f and photosystem I in the chlorophyll d-dominated cyanobacterium, *Acaryochloris marina*, *J. Biol. Chem.* 283 (2008) 25218–25226.
- [23] S.I. Allakhverdiev, et al., Redox potential of pheophytin a in photosystem II of two cyanobacteria having the different special pair chlorophylls, *Proc. Natl. Acad. Sci. USA* 107 (2010) 3924–3929.
- [24] J. Feitelson, D. Mauzerall, Wide-band, time-resolved photoacoustic study of electron-transfer reactions: photoexcited magnesium porphyrin and quinones, *J. Phys. Chem.* 97 (1993) 8410–8413.
- [25] Y. Cha, D. Mauzerall, Energy storage of linear and cyclic electron flows in photosynthesis, *Plant Physiol.* 100 (1992) 1869–1877.
- [26] D. Charlebois, D. Mauzerall, Energy storage and optical cross-section of PS I in the cyanobacterium *Synechococcus PCC 7002* and a *psaE*[−] mutant, *Photosynth. Res.* 59 (1999) 27–38.
- [27] D.C. Mauzerall, Determination of oxygen emission and uptake in leaves by pulsed, time resolved photoacoustics, *Plant Physiol.* 94 (1990) 278–283.
- [28] R.D. Britt, in: D.R. Ort, C.F. Yocum (Eds.), Oxygenic Photosynthesis: The Light Reactions, Kluwer, Dordrecht, 1996, pp. 139–164.
- [29] R.E. Blankenship, R.C. Prince, Excited-state redox potentials and the Z scheme of photosynthesis, *Trends Biochem. Sci.* 10 (1985) 382–383.
- [30] F. Rappaport, M. Guergova-Kuras, P.J. Nixon, B.A. Diner, J. Lavergne, Kinetics and pathways of charge recombination in photosystem II, *Biochemistry* 41 (2002) 8518–8527.
- [31] D. Noy, C.C. Moser, P.L. Dutton, Design and engineering of photosynthetic light-harvesting and electron transfer using length, time, and energy scales, *Biochim. Biophys. Acta* 1757 (2006) 90–105.
- [32] T. Tomo, et al., Identification of the special pair of photosystem II in a chlorophyll d-dominated cyanobacterium, *Proc. Natl. Acad. Sci. USA* 104 (2007) 7283–7288.
- [33] Y. Song, J. Mao, M.R. Gunner, MCCE2: Improving protein pK_a calculations with extensive side chain rotamer sampling, *J. Comput. Chem.* (2009), doi:10.1002/jcc.21222.
- [34] M.L. Groot, et al., Initial electron donor and acceptor in isolated photosystem II reaction centers identified with femtosecond mid-IR spectroscopy, *Proc. Natl. Acad. Sci. USA* 102 (2005) 13087–13092.
- [35] A.R. Holzwarth, et al., Kinetics and mechanism of electron transfer in intact photosystem II and in the isolated reaction center: pheophytin is the primary electron acceptor, *Proc. Natl. Acad. Sci. USA* 103 (2006) 6895–6900.
- [36] M. Kobayashi, S. Ohashi, K. Iwamoto, Y. Shiraiwa, Y. Kato, T. Watanabe, Redox potential of chlorophyll d in vitro, *Biochim. Biophys. Acta* 1767 (2007) 596–602.